Nat. Volatiles & Essent. Oils, 2021; 8(5): 13429-13444

NVEO
Natural Volatiles &
Essential Oils

Punching Shear Behaviour Of Restrained Two Way Slabs With Gfrp As Replacement To Steel Bars

Hanumesh B M[1] , N.Venkata Ramana[2] and H.R Prabhakara[3]

[1] Research scholar, Department of Civil Engineering, Visvesvaraya Technological University, GM Institute of Technology, Davangere, Karnataka-577006, India.

[2 and 3] Associate Professor and Professor, Civil Engineering Department, Visvesvaraya Technological University, UBDT CE, Davangere, Karnataka-577004, India.

Abstract

An experimental investigation was carried out on two-way slab elements, and elements are reinforced with hybrid reinforcements of Steel and Glass Fiber Reinforced Polymer (GFRP) bars. The GFRP reinforcement is provided in the slab as a replacement for steel in the proportions of 0, 28.57, 57.14, 85.71, and 100%. A total of fifteen slabs are cast for five replacements, and the slabs are tested under punching shear to evaluate failure loads, stiffness, energy absorption, and load-deflection characteristics. The slabs with hybrid reinforcements showed superior performance compared with slab 100%GFRP reinforcement. IS 456 and ACI 318 guidelines are considered to assess failure loads, and those were underestimated the results. To predict the failure loads regression model is proposed in this article, and its performance provided satisfactory results.

Keywords: Restrained Two-way slab, Punching shear, GFRP, and Steel reinforcements, Cracking and Failure loads, stiffness and energy absorption, a mathematical model

1. Introduction

Nowadays, reinforced concrete flat slabs are widely used for commercial and public office buildings. It is simple during construction and electrification and leads to less formwork cost. On the other hand, these flat slabs are more sensitive to punching shear; in this aspect, many techniques improve the strengths. Many strengthening techniques are associated with steel material in continuous and discontinuous reinforcement. The improved methods are viable during the construction of flat slabs and, theoretically, also it is well established. From the past literature, it is well said that the steel material is susceptible to corrosion as time progresses. Many anti-corrosion techniques are advised based on laboratory and actual observations to minimize the corrosion of steel reinforcement. Concern for this, polymer materials were induced for the construction industry as an alternative material for steel reinforcement in recent decades. The fiber reinforced polymer (FRP) materials are in the form of continuous and discontinuous reinforcement (in the form of fibers). The available FRP materials are glass, basalt, carbon, and aramid. The FRP rods are prepared with fibers and polymer; the fibers are embedded in the polymers (epoxies, vinyl, and polyesters). The fibers and polymers individually do not serve the function of structural material, whereas, in combination, it may be possible to attain structural part. After adding the fibers for polymers, a little mass is volatile and forms a good bond between the matrixes. It is possible to fabricate material in the required shape (solid, round and hollow, and other shapes). The present investigation is aimed to know the punching shear behaviour of two-way slabs reinforced with steel and glass fiber reinforced polymer (GFRP) bars. In the concern the past research works appeared on this arena is furnishing herein.

N. Banthia et al. (1995) studied the behaviour of concrete slabs reinforced with FRP and steel grids and noticed that the ultimate loads of FRP reinforced slabs were equal to or higher than that reinforced with steel bars. **Stijn Matthys and Luc Taerwe (2000)** investigated the behaviour of one-way slabs reinforced with FRP bars under concentrated loading. With the increased reinforcement ratio and increased slab depth, the punching shear strength was similar to or higher than steel-reinforced reference slabs. **T. Hassan et al. (1999)** studied two categories of slabs: reinforced with CFRP and other slabs reinforced with steel and GFRP bars. The authors recommended using CFRP and GFRP reinforcement for bridge deck slabs based on serviceability conditions and reinforcement ratios. **Abdel Wahab El-Ghandour et al. (2003)** investigated the punching shear behaviour of FRP RC flat slabs with and without CFRP shear reinforcement. The results showed that CFRP shear reinforcement was inefficient in enhancing the strength of slabs due to brittleness. **Sherif El-Gamal et al. (2005)** investigated the punching shear behaviour of CFRP and GFRP reinforced slabs and compared results with the slab reinforced with steel bars. The experimental result shows that the maximum deflection measured was below the allowable code limits. **Haitang Zhu et al. (2010)** conducted an experimental investigation on Basalt Fiber Reinforced Polymer (BFRP) reinforced two-way simply supported slabs. The load-deflection curve of the slabs depends on concrete strength, location of the concentrated load, and FRP reinforcement ratios. **K. H. Min et al. (2010)** observed the behaviour of FRP reinforced and Steel fiber reinforced slabs under flexure & punching load. The results showed that the FRP strengthening system performed well under punching loads. **K. Bouguerra et al. (2011)** investigated the behaviour of bridge deck slabs reinforced with FRP bars. The results highlight the crack width as it depended on bottom transverse reinforcement ratios. **Long Nguyen-Minh and Marian Rovank (2013)** varied the reinforcement ratio in GFRP reinforced flat slabs and noticed a 36% increase in punching shear resistance with a reduction in deflections of 35%. **Mohamed Hassan et al. (2013)** studied the effect of GFRP bars in the slabs, and their study reported that with increasing the reinforcement provision in slabs, punching shear capacities were enhanced with lower deflections. **Gobithas Tharmarajah et al. (2014),** through their research, proved that GFRP and BFRP are good alternatives to steel in restrained slabs. **Fareed Elgabbas et al. (2016)** have reported the effect of BRFRP bars in the slab elements; the specimens are tested for punching shear. From the findings, it is understood that there is not much effect of support reinforcement to exhibit the performance compared to a slab without support BFRP bars. **Ahmed Gouda and Ehab El-Salakawy (2015)** studied slab column connections reinforced with GFRP and showed that GFRP- RC connection rigidity is similar to steel RC connection with comparable deflection and capacity at failure. **Asghar Vatani Oskouei et al. (2017)** studied the performance of lightweight concrete footings reinforced with GFRP. The results show that crack width in lightweight concrete footings was wider than in normal-weight concrete footings. **Sadjad Amir Hemzah et al. (2019)** observed that yield lines due to punching shear were affected by the shape of the column in punching shear. From the above observations, it came to know that attention was not focused on hybrid reinforced slab elements tested for punching shear. Hence to know the performance of hybrid reinforcement (GFRP and Steel) in punching shear, an experimental program is planned, and its description is shown below.

2.0 Experimental program

2.1 Test specimens

To evaluate the performance of hybrid reinforcements two-way slab elements experiment was planned with five combinations of steel and GFRP. The slab elements are cast with dimensions of 600x600x75mm, and for each combination of GFRP and Steel, three slab elements are cast; in total, the number of slabs is 15. The plan geometry dimensions give the span ratio as 1, and the slab is provided with a clear cover of 15mm. The reinforcement ratio in the slab element was arbitrarily provided as 1.22% (it satisfies the minimum and maximum requirements of IS456 and ACI318 code provisions). This percentage of reinforcement is fulfilled with 7 number of 10mm diameter bars in each direction. At support, reinforcement is provided identically with bottom reinforcement except for the extension of the bar, the bar provided for a length of 100mm from the support. This arrangement helps to bear the negative moment for the restrained slab element at all four edges. Out of the total of 7 numbers of bars in each direction, the steel bars are replaced with GFRP as 0, 2,4,6,7. It gives the percentage as 0%G+100%S, 28.57%G+71.43%S, 57.14%G+42.86%S, 85.71%G+14.29%S, and 100%G+0%S (G indicates GFRP bar and S indicates Steel bar).

2.2 Material properties, casting and curing of slab elements

Portland Pozzolana cement conforming to IS 1489-(Part 1), fine and coarse aggregate conforming to IS383, and portable water was used for the experimental study. Related to GFRP and Steel reinforcements, the GFRP was procured from Go-Green products, Chennai, India, and steel reinforcement were procured from a local source. The properties of GFRP and Steel reinforcements are shown in Table 1. The concrete mix is designed for M20 grade concrete, concerning IS10262 guidelines. Finally, the mix has arrived as 1:1.64:2.87 with a water-cement ratio of 0.5. All the slab specimens are cast with the arrived mix, and cast specimens are kept in water for 28 days, later shifted for experimentation. The detailed casting procedure and curing of specimens can be viewed in figure 1.

Table 1: Physical properties of Steel and GFRP bars

Sl. No	Property	Steel bar	GFRP bar
1	Dia of bar	10mm	10mm
2	Cross section area (mm^2)	78.55	78.55
3	Weight (Kg/m)	0.62	0.1
4	Modulus of Elasticity (MPa)	$2x10^5$	50,000
5	Bending strength (MPa)	415	627

	
Dry mixing of ingredients	**Wet mixing of ingredients**
	
GS1 Slab Bottom mat	**GS1 Slab Top mat**
	
GS2 Slab Bottom mat	**GS2 Slab Top mat**
	

GS3 Slab Bottom mat	GS3 Slab Top mat
	
GS4 Slab Bottom mat	**GS4 Slab Top mat**
	
GS5 Slab Bottom mat	**GS5 Slab Top mat**
	
Concreting	**Compaction with needle vibrator**

Cast specimens Compaction

Curing of Slab Specimens

Figure 1: Casting and curing of slab specimens

2.3 Test procedure

After completing the 28-day curing period, the slab is kept ready for testing. First, the slab is placed on the testing platform to simulate the fixidity nut and bolt system. A total of 12 bolts are used to arrive at this condition; the bots are tightly fitted for the slab with the help of a stripper plate. After this process, to simulate punching shear mode, a solid steel rod (50mm) and a welded steel plate (100x100x25mm) were placed on the slab surface. One side of the steel rod is attached with a hydraulic jack and a proving ring (1000kN capacity). Load is progressed on this with an increment of 2kN, and for every increment, deflection is recorded with centrally placed LVDT (Linear variable differential transformer (most minor count of LVDT is 0.1mm), in addition, at first crack and ultimate stages deflections, are recorded. The testing arrangement for the slab element can be viewed in figure 2.

Figure 2: Test set up for testing of slab specimen

3.0 Discussion of Test Results

3.1 Failure loads

The failure loads for two-way slab elements are presented in Table 2. The table shows that punching shear strength decreases as the GFRP reinforcement increases in the slab element. The slab with 100%GFRP reinforcement showed lesser strength than the slab with 100% steel reinforcement. The GS2 slab showed an increase in its strength of 29.41% compared with the GS1 slab. The other slabs, GS3 and GS4, showed a rise in first crack loads of about 47.06 and 70.59% compared with the GS1 slab. The GS5 slab showed an increase of the strength of 91.18% compared with the GS1 slab. From all the above observations, the slab with steel reinforced showed its superiority with the combination of GFRP and Steel and exclusively with GFRP reinforcement. Similar to first crack behaviour, all hybrid reinforced slabs showed the same trend at ultimate loads. The GS1 slab showed failure loads of 160kN, and the GS5 slab showed a failure load of 252kN, and its strength increment is 57.50% compared with the GS1 slab specimen. The GS3, GS4 slabs showed an increment of 31.25 and 43.75% strength, respectively, compared with the GS1 slab. The failure loads at the first crack and ultimate stages slab with steel reinforcement showed superior performance to the GFRP reinforced slab. It may be due to the differences in modulus of elasticities. The steel reinforcement has more modulus of elasticity (2×10^5MPa) than the GFRP reinforcement (50×10^3MPa), and their ratio is 0.25.

Table 2: Failure loads

Sl. No	Nomenclature of slab	Number of bars in slab with GFRP and Steel	% of hybrid Reinforcement	First crack load (kN)	Ultimate load (kN)
1	GS1	7G+0S	100%G+0%S	68	160
2	GS2	6G+1S	85.71%G+14.29%S	88	180
3	GS3	4G+3S	57.14%G+42.86%S	100	210
4	GS4	2G+5S	28.57%G+71.43%S	116	230
5	GS5	0G+7S	0%G+100%S	130	252

3.2 Load Deflection response

The load-deflection of hybrid reinforced slabs elements are shown in figure 1, and the deflections at first crack and ultimate failure loads are shown in Table 3. The figure shows that the slab specimens showed linearity before the first crack load. Later, non-linearity is exhibited in the load-deflection path as the load increases. For the slabs with 100%GFRP to 100%Steel reinforcement, the deflections at first crack and ultimate loads vary from 2.2 to 3.2mm and 8.8 to 11.3mm, respectively. As the %GFRP reinforcement decreases in hybrid reinforced slab specimens, the deflections and the load capacities are increased, and also it reflects on post crack yielding (it ranges from 6.6 to 8.1mm). This observation led to the slab with steel reinforcement showing superior to the slab with GFRP reinforcement. The ductility ratios are different for different hybrid reinforced slab elements (varied from 4.00 to 3.53), as shown in Table 2. This variation is because the GFRP material has a brittle nature compared to steel reinforcement. The steel has identical properties in all directions, but it is not so in GFRP bars.

Table 3: Deflections at first crack and ultimate loads stages

Sl. No	Nomenclature of slab	Number of bars in slab with GFRP and Steel	% of hybrid Reinforcement	Deflection at first crack (mm)	Deflection at ultimate Load (mm)	Post crack Yielding (mm)	Ductility Ratio
1	GS1	7G+0S	100%G+0%S	2.2	8.8	6.6	4.00
2	GS2	6G+1S	85.71%G+14.29%S	2.6	9.3	6.7	3.58
3	GS3	4G+3S	57.14%G+42.86%S	2.7	10.2	7.5	3.78
4	GS4	2G+5S	28.57%G+71.43%S	2.9	10.8	7.9	3.72
5	GS5	0G+7S	0%G+100%S	3.2	11.3	8.1	3.53

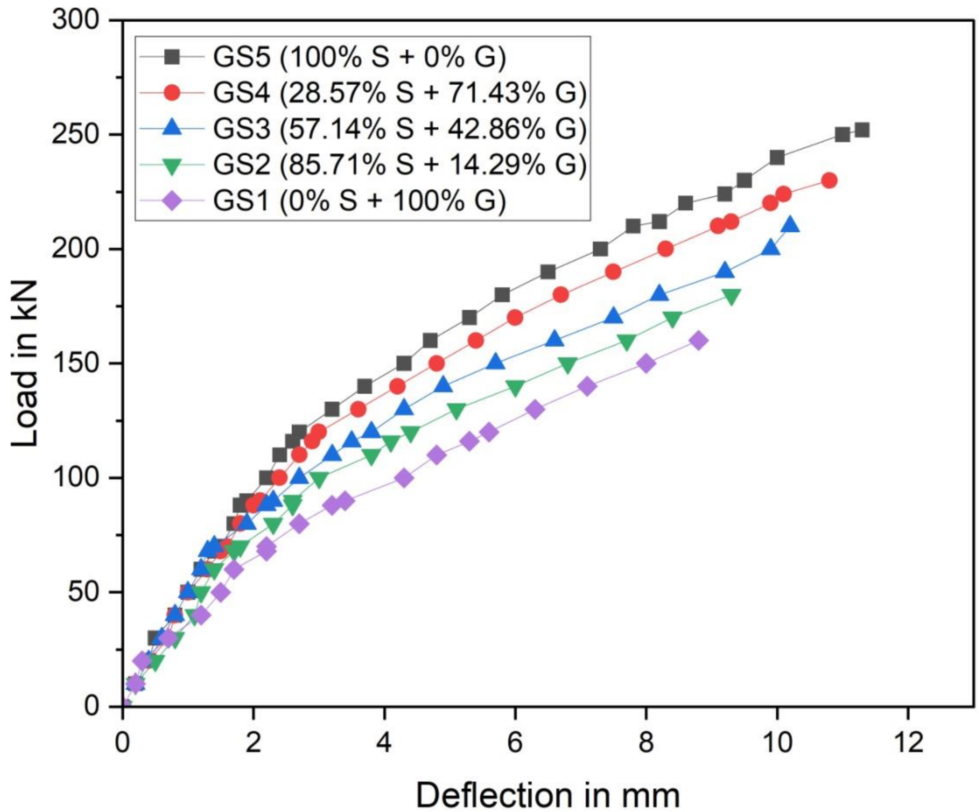

Figure 3: Load deflection for different slab specimens

3.3 Stiffness and Energy absorption

Stiffness for hybrid reinforced slab elements is shown in Table 4, and from the table, it is observed that, as the GFRP reinforcement decreases, the stiffness increases at the first crack stage and varies from 30.91 to 40.3kN/mm. As a result, the GS2, GS3, GS4, and GS5 slabs show a higher percentage of stiffness of 9.51, 19.83, 29.41, and 31.45 %, respectively, compared with the GS1 slab specimen. And at the ultimate failure stage, slab elements show differences among the slab specimens. At this stage, the GS2, GS3, GS4, and GS5 slabs show different percentages of stiffness of 6.44, 13.26, 17.16, and 22.66%, respectively, compared with the GS1 slab specimen. By comparing the stiffness at the first crack stage and ultimate stages, it is observed that stiffness is more numeric at the first crack stage than at the ultimate stage.

Table 4: Stiffness at first crack and ultimate load stages

Sl. No	Nomenclature of slab	Number of bars in slab with	% of hybrid Reinforcement	Stiffness at first crack load (kN/mm)	Stiffness at ultimate load (kN/mm)

		GFRP and Steel			
1	GS1	7G+0S	100%G+0%S	30.91	18.18
2	GS2	6G+1S	85.71%G+14.29%S	33.85	19.35
3	GS3	4G+3S	57.14%G+42.86%S	37.04	20.59
4	GS4	2G+5S	28.57%G+71.43%S	40.00	21.30
5	GS5	0G+7S	0%G+100%S	40.63	22.30

Energy absorption for hybrid reinforced slab specimens is provided in Table 5. The results show that, as the GFRP reinforcement decreases in place of hybrid reinforcement, the energy absorption increases at the first crack and ultimate load stages. For example, at the first crack load stages, the energy absorption for GS2, GS3, GS4, and GS5 slab specimens showed an increment of 47.81, 84.06, 112.19, and 172.50% compared to the GS1 slab. Similarly, at the ultimate load stage, the identical slab specimens are showed an increment of 22.32, 54.39, 84.81, and 112.60% compared with the GS1 slab.

Table 5: Energy absorption

Sl. No.	Nomenclature of slab	Number of bars in slab with GFRP and Steel	% of hybrid Reinforcement	Up to First Crack Load		Up to Failure Load	
				Energy absorption (kN mm)	Energy absorption per unit volume (kJ/m^3)	Total energy absorption (kN mm)	Total energy absorption per unit volume (kJ/m^3)
1	GS1	7G+0S	100%G+ 0%S	86.5	3.20	863.7	31.99
2	GS2	6G+1S	85.71%G+14.29%S	127.8	4.73	1056.6	39.13
3	GS3	4G+3S	57.14%G+42.86%S	158.9	5.89	1333.7	49.39
4	GS4	2G+5S	28.57%G+S71.43%S	183.5	6.79	1595.9	59.12
5	GS5	0G+7S	0%G+ 100%S	235.4	8.72	1836.3	68.01

3.4 Crack pattern

During the experimentation of slab specimens, crack/s initialization is observed at the bottom of the slab (near the load point). Their propagations are noticed along with load enhancement on the slab specimen. With the increase of loads, the cracks are travelled towards supports, and thereby, the cracks are geometry radial. After attaining the ultimate loads for all the slab specimens, the specimens are taken out from the testing loading platform for observations of the whole crack pattern, as shown in figure 4.

	
Top view of Loading	**GS1 bottom face**
	
GS2 bottom face	**GS3 bottom face**
	
GS4 bottom face	**GS5 bottom face**

Figure 4: Tested Slab specimens

3.5 Comparison of experimental results with existing codes

In the absence of code guidelines for hybrid reinforced slabs in punching shear, the methods specified in the major building codes of IS 456-2000 and ACI 318-2011 are considered in the present study. However, the above two building code methods may not apply to the current work because the slabs are reinforced with hybrid reinforcements. Both IS, and ACI codes do not address the reinforcement in the slab element. However, they have generally been provided for conventional reinforcement of steel. In this context, the above-said codes are to be tested for their validity herein. About this, the detailed discussions along with the calculations are presented below.

1. As per Indian Standard Plain and Reinforced Concrete- Code of Practice (IS 456 – 2000)

The IS456 code has been provided with the following equation to calculate the punching shear strength (Vc)

$V_C = k_s \tau_u b_0 d$

Where

$k_s = (0.5 + \beta_c) \leq 1$

$\tau_u = 0.25 \sqrt{f_{ck}}$ MPa

Where

V_C = Punching shear strength (kN)

b_o = Critical perimeter at a distance of 0.5d from the column face (mm)

d = Effective slab depth (mm)

f_{ck} = Concrete-cube compressive strength (MPa) after 28 days

β_c = Ratio of the long side to the short side of the concentrated load or reaction area

τ_u = Shear strength of concrete in Mpa

The IS456 code has been provided the following equation to calculate the punching shear strength (Vc)

$V_C = k_s \tau_u b_0 d$

Where

d = 75-20 mm = 55 mm

b_o = ((0.5 x (75-20) x 2)+100) x 4 = 620 mm

f_{ck} = 27.5 MPa

β_c = 1

$k_s = (0.5 + \beta_c) \leq 1 = (0.5 + 1) \leq 1 = 1$

$\tau_u = 0.25 \sqrt{f_{ck}}$ MPa = $0.25 \sqrt{27.5}$ MPa = 1.31MPa

So,

$V_C = k_s \tau_u b_0 d$

V_C = 1 x 1.31 x 620 x x 55

V_C = 44.67 kN

2. As per American Concrete Institute (ACI 318 -2011)

According to ACI 318 (2011), the design punching strength is taken as lest of the following to estimate the punching shear strength

$$V_c = \left(2 + \frac{4}{\beta_c}\right)\frac{\sqrt{f_{ck}}\, u\, d}{12}\gamma_c$$
$$V_c = \left(2 + \frac{\alpha_s d}{u}\right)\frac{\sqrt{f_{ck}}\, u\, d}{12}\gamma_c$$
$$V_c = \frac{1}{3}\sqrt{f_{ck}}\, u\, d\, \gamma_c$$

Where

V_c = Punching shear strength (kN)

β_c = ratio of the long side to the short side of the concentrated load or reaction area

f_{ck}= 28 days concrete-cylinder compressive strength (MPa)

α_s = Parameter that depends on columns geometry (40 for inner columns)

u = basic control perimeter at a distance of 0.5d from the columns border/ face

d = effective slab depth

γ = Concrete material partial factor (0.75)

According to ACI 318 (2011), the design punching shear strength (Vc) is taken as lest of the following to estimate the punching shear strength

$$V_c = \left(2 + \frac{4}{\beta_c}\right)\frac{\sqrt{f_{ck}}\, u\, d}{12}\gamma_c$$
$$V_c = \left(2 + \frac{\alpha_s d}{u}\right)\frac{\sqrt{f_{ck}}\, u\, d}{12}\gamma_c$$
$$V_c = \frac{1}{3}\sqrt{f_{ck}}\, u\, d\, \gamma_c$$

Where

β_c = 1

f_{ck}= 22.89 (MPa)

α_s = 40

u = ((0.5 x (75-20) x 2)+100) x 4 = 620 mm

d = 75-20 mm = 55 mm

γ = 0.75

$$V_c = \left(2 + \frac{4}{1}\right)\frac{\sqrt{22.89} \times 620 \times 55}{12} \times 0.75 = 61.18\ \mathrm{kN}$$
$$V_c = \left(2 + \frac{40 \times 55}{620}\right)\frac{\sqrt{22.89} \times 620 \times 55}{12} \times 0.75 = 56.57\ \mathrm{kN}$$
$$V_c = \frac{1}{3}\sqrt{22.89} \times 620 \times 55 \times 0.75 = 40.79\ \mathrm{kN}$$

The third equation gives the least value of punching shear. So, $V_c = 40.79\ \mathrm{kN}$

The computations of ultimate loads by IS and ACI codes have been presented in Table 6. Moreover, the ratios between experimental to code provisions shown loads are furnished in the same table, and results show that an average experimental to IS and ACI provided 4.67 and 5.13. Hence, it is needed to develop a model to estimate with good accuracy and consider the effect of percentage GFRP reinforcement.

Table 6: Summary of the calculated punching shear strengths based on various codes

Sl. No	Nomenclature of slab	Number of bars in slab with GFRP and Steel	% of hybrid Reinforcement	Ultimate load (kN) [EXP]	IS456-2000 Ultimate Punching shear load (kN)	ACI 318 Ultimate Punching shear load (kN)	EXP/ IS	EXP /ACI
1	GS1	7G+0S	100%G+ 0%S	160	44.67	40.79	3.58	3.92
2	GS2	6G+1S	85.71%G+14.29%S	180			4.30	4.41
3	GS3	4G+3S	57.14%G+42.86%S	210			4.70	5.15
4	GS4	2G+5S	28.57%G+S71.43%S	230			5.15	5.64
5	GS5	0G+7S	0%G+ 100%S	252			4.64	6.18
Average ratio							4.67	5.13

3.6 Regression model and its performance

To predict the experimental results in this section, a regression model has been proposed with a regression coefficient of 0.87478, and the performance is also checked and presented in Table 7. The table shows that the experimental and regression model ratio varied with a maximum of 17%. Hence the proposed model can be used to estimate experimental results satisfactorily.

$$P_u = [1.35 - (0.33 \times \%GFRP)] \sqrt{fck}\, b_o\, d$$

Where,
%GFRP = GFRP reinforcement in percentage (replacement to steel reinforcement)
f_{ck} =28 days cube compressive strength (MPa)
b_o = Critical perimeter at a distance of 0.5d from the column face (mm)
d = Effective depth of slab (mm)

Table 7: Performance of regression model

Sl. No.	Nomenclature of slab	Number of bars in slab with GFRP and Steel	% of hybrid Reinforcement	EXP (kN)	RM (kN)	EXP/RM
1	GS1	7G+0S	100%G+ 0%S	252	241.41	1.04
2	GS2	6G+1S	85.71%G+14.29%S	230	224.55	1.02
3	GS3	4G+3S	57.14%G+42.86%S	210	207.69	1.01
4	GS4	2G+5S	28.57%G+S71.43%S	180	190.83	0.94
5	GS5	0G+7S	0%G+ 100%S	160	182.39	0.87

4.0 Conclusions

The slabs with hybrid reinforcements showed superior performance compared with 100%GFRP slabs. The ultimate punching shear strength of a 100%GFRP reinforcement slab is 57.50% of the 100% steel reinforced slab. The slabs with 85.17, 57.14,28.57 and 0% GFRP reinforcement (as replacement to steel reinforcement) showed an increase of 29.41,47.06,70.59 and 91.18% at first crack and 12.50,31.25,43.75 and 57.50% at ultimate failure state in punching shear compared to 100%GFRP reinforced slab. Similarly, the same slabs increased total energy absorption by 22.32, 54.39, 84.81, and 112.60% compared to the 100%GFRP slab. For 0 to 100% GFRP slab specimens, the stiffness at ultimate loads decreases from 23.30 to 18.18kN/mm. The punching shear strengths for all slabs are evaluated with IS 456 and ACI 318 code provisions and found inconsistency with test results. A model is proposed to assess the test results in this, and its suitability is checked; the model has shown satisfactory results.

References

1. A. Gouda and E. El-Salakawy, "Punching Shear Strength of GFRP-RC Interior Slab–Column Connections Subjected to Moment Transfer," J. Compos. Constr., vol. 20, no. 1, p. 04015037, 2016, doi: 10.1061/(ASCE)cc.1943-5614.0000597.
2. A. V. Oskouei, M. P. Kivi, H. Araghi, and M. Bazli, "Experimental study of the punching behaviour of GFRP reinforced lightweight concrete footing," Mater. Struct. Constr., vol. 50, no. 6, 2017, doi: 10.1617/s11527-017-1127-2.
3. A. W. El-Ghandour, K. Pilakoutas, and P. Waldron, "Punching Shear Behavior of Fiber Reinforced Polymers Reinforced Concrete Flat Slabs: Experimental Study," J. Compos. Constr., vol. 7, no. 3, pp. 258–265, 2003, doi: 10.1061/(asce)1090-0268(2003)7:3(258).
4. ACI 318:2011 – Building Code Requirements for Structural Concrete and Commentary
5. D. Eck, "and U Ltimate L Oad B Ehavior of B Ridge," vol. 45, no. February, pp. 16–23, 2000.
6. E. El-Salakawy and B. Benmokrane, "Serviceability of concrete bridge deck slabs reinforced with fibre-reinforced polymer composite bars," ACI Struct. J., vol. 101, no. 5, pp. 727–736, 2004, doi: 10.14359/13395.
7. F. Elgabbas, E. A. Ahmed, and B. Benmokrane, "Experimental Testing of Concrete Bridge-Deck Slabs Reinforced with Basalt-FRP Reinforcing Bars under Concentrated Loads," J. Bridg. Eng., vol. 21, no. 7, p. 04016029, 2016, doi: 10.1061/(ASCE)be.1943-5592.0000892.
8. Gobithas Tharmarajah, Susan E. Taylor, David J. Cleland and Des Robinson, "Corrosion-Resistant FRP Reinforcement for bridge deck slabs", ICE, 2014, PP. 208-217.
9. H. Zhu, Y. Zhang, D. Gao, and Z. Xiao, "Deformation behaviour of concrete two-way slabs reinforced with BFRP bars subjected to eccentric loading," Adv. FRP Compos. Civ. Eng. - Proc. 5th Int. Conf. FRP Compos. Civ. Eng. CICE 2010, pp. 296–300, 2011, doi: 10.1007/978-3-642-17487-2_63.
10. IS 10262: 2009 - Concrete Mix Proportioning Guidelines
11. IS 1489-(Part 1) -1991- Portland Pozzolana Cement Specification Part 1 Fly Ash Based
12. IS 383 – 2016 – Coarse and Fine Aggregate for Concrete - Specification
13. IS 456:2000 – Plain and Reinforced Concrete – Code of Practice
14. K. Bouguerra, E. A. Ahmed, S. El-Gamal, and B. Benmokrane, "Testing of full-scale concrete bridge deck slabs reinforced with fiber-reinforced polymer (FRP) bars," Constr. Build. Mater., vol. 25, no. 10, pp. 3956–3965, 2011, doi: 10.1016/j.conbuildmat.2011.04.028.

15. K. H. Min, J. M. Yang, D. Y. Yoo, and Y. S. Yoon, “chp%3A10.1007%2F978-3-642-17487-2_89.pdf,” pp. 2–6, 2011.
16. L. Nguyen-Minh and M. Rovňák, "Punching Shear Resistance of Interior GFRP Reinforced Slab-Column Connections," J. Compos. Constr., vol. 17, no. 1, pp. 2–13, 2013, doi: 10.1061/(asce)cc.1943-5614.0000324.
17. M. Hassan, E. Ahmed, and B. Benmokrane, "Punching-Shear Strength of Normal and High-Strength Two-Way Concrete Slabs Reinforced with GFRP Bars," J. Compos. Constr., vol. 17, no. 6, p. 04013003, 2013, doi: 10.1061/(asce)cc.1943-5614.0000424.
18. N. Banthia, M. AI-Asaly and S. Ma, "Behavior of Concrete Slabs Reinforced with Fiber-Reinforced Plastic Grid", Journal Of Materials In Civil Engineering I November 1995, pp. 252-257.
19. S. El-Gamal, E. El-Salakawy, and B. Benmokrane, "Influence of Reinforcement on the Behavior of Concrete Bridge Deck Slabs Reinforced with FRP Bars," J. Compos. Constr., vol. 11, no. 5, pp. 449–458, 2007, doi: 10.1061/(ASCE)1090-0268(2007)11:5(449).
20. S. Lecturer, I. Technology, S. Lanka, and S. Lecturer, "Corrosion-resistant FRP," vol. 168, 2015.
21. S. T. L. Matthys, "Concrete Slabs Reinforced with FRP Grids.," J. Compos. Constr., vol. 4, no. August, pp. 154–161, 2000.
22. Sadjad Amir Hemzah, Salam Al-Obaidi and Thulfiqar Salim, "Punching Shear Model for Normal and High-Strength Concrete Slabs Reinforced with CFRP or Steel Bars", Jordan Journal of Civil Engineering, Vol. 13, No. 2, 2019, pp. 250-268.
23. T. Hassan, A. Abdelrahman, G. Tadros, and S. Rizkalla, "Fibre reinforced polymer reinforcing bars for bridge decks," Can. J. Civ. Eng., vol. 27, no. 5, pp. 839–849, 2000, doi: 10.1139/l99-098.
24. Kumar, S. (2022). Strategic management of carbon footprint using carbon collectible non-fungible tokens (NFTS) on blockchain. Academy of Strategic Management Journal, 21(S3), 1-10
25. Kumar, S. (2021). Review of geothermal energy as an alternate energy source for Bitcoin mining. Journal of Economics and Economic Education Research, 23(1), 1-12
26. Ritika Malik, Aarushi Kataria and Naveen Nandal, Analysis of Digital Wallets for Sustainability: A Comparative Analysis between Retailers and Customers, International Journal of Management, 11(7), 2020, pp. 358-370.
27. Aarushi, Naveen Nandal, Parul Agrawal. AN EXPLORATORY RESEARCH IN PRODUCT INNOVATION IN AUTOMOBILE SECTOR. JCR. 2020; 7(2): 522-529. doi:10.31838/jcr.07.02.98